Cluster-collision frequency. I. The long-range intercluster potential

A. S. Amadon and W. H. Marlow*

Department of Nuclear Engineering, Texas A&M University, College Station, Texas 77843-3133
(Received 24 September 1990)

In recent years, gas-borne atomic and molecular clusters have emerged as subjects of basic physical and chemical interest and are gaining recognition for their importance in numerous applications. To calculate the evolution of the mass distribution of these clusters, their thermal collision rates are required. For computing these collision rates, the long-range interaction energy between clusters is required and is the subject of this paper. Utilizing a formulation of the iterated van der Waals interaction over discrete molecules that can be shown to converge with increasing numbers of atoms to the Lifshitz–van der Waals interaction for condensed matter, we calculate the interaction energy as a function of center-of-mass separation for identical pairs of clusters of 13, 33, and 55 molecules of carbon tetrachloride in icosahedral and dodecahedral configurations. Two different relative orientations are chosen for each pair of clusters, and the energies are compared with energies calculated from the standard formula for continuum matter derived by summing over pair interactions with the Hamaker constant calculated according to Lifshitz theory. The results of these calculations give long-range interaction energies that assume typical adhesion-type values at cluster contact, unlike the unbounded results for the Lifshitz-Hamaker model. The relative difference between the discrete molecular energies and the continuum energies vanishes for $r^* \approx 2$, where r^* is the center-of-mass separation distance in units of cluster diameter. For larger separations, the relative difference changes sign, showing a value of approximately 15%, with the difference diminishing for increasing-sized clusters. We argue that the details of the results of these calculations indicate that the deficiency in the continuum picture for small separations lies in the substitution of an averaged picture of the interaction for what is intrinsically the cumulative energy of discrete interactants.

I. INTRODUCTION

Gas-borne clusters spanning the range from atomic to macroscopic dimensions enter questions as diverse as condensed-matter research, air pollution, and environmental chemistry, and many areas of technology from combustion to vapor deposition. Wherever they appear, the evolution of their mass distributions is dependent upon their thermal-collision rates. However, the dependences of cluster-collision rates on their physical properties apparently has not been systematically treated. The development of a framework for calculating both the evolving physical properties that affect cluster collisions and the utilization of those properties in practical collision-rate calculations raises questions of intrinsic physical interest as well as of importance for their applications to modeling cluster behavior in many different fields.

In the simplest example, which is the subject of these papers, a cluster of n monomers $\mathcal{C}_n$ has a unique configuration and coagulates with a cluster of m monomers $\mathcal{C}_m$ to produce a cluster of $p = n + m$ monomers, $\mathcal{C}_n + \mathcal{C}_m \rightarrow \mathcal{C}_p$, with the population balance equations written as

$$\frac{d[\mathcal{C}_p]}{dt} = \frac{1}{2} \sum_{\substack{n \ m \\ m+n=p}} k_{nm}[\mathcal{C}_n][\mathcal{C}_m] - [\mathcal{C}_p]\sum_{i=1} k_{pi}[\mathcal{C}_i] \ .$$

Here, the brackets [ ] denote concentration, t is time, and k_{nm} is the rate of the coagulation reaction. The coagulation rate can be divided into two factors: a sticking probability and a collision rate which is the subject of the following paper.[1]

To understand what might comprise the minimal set of factors required for calculating k_{nm}, a comparison with the limiting cases that "bracket" clusters is helpful. The reaction rate for two interacting gas molecules is dependent upon a number of factors, including physical structure, temperature, the presence of a third body, and electronic states.[2] In contrast, in the "macroscopic" limit, which is here taken to be ultrafine aerosol particles in the free-molecular transport regime (defined as particles of radii much smaller than gas mean free path),[3] the dependences of the rate are generally much simpler than for molecules for several reasons: First, "condensed" bodies, even in the nanometer range, possess a large number of vibrational modes which readily thermalize the collisional kinetic energy, as demonstrated by simulation calculations.[4] Thus, in this case the collisional energy is effectively dissipated into heat so that particle-particle collisions are inelastic. The onset of this characteristic of irreversibility in aerosol collisions has been proposed in a dynamically based definition of an aerosol system[5] as opposed to the many functional definitions in the literature.[6] Second, there is always an attractive interaction energy between condensed bodies, separated by a vacuum, resulting from the collective effects of long-range, or van

der Waals, intermolecular potentials.[7] This energy has the dual effect of enhancing the collision cross section of the particles beyond their geometrical cross section[8,9] and of overriding the short-range repulsion that may develop as the surface atoms of the particles approach. Finally, for the overall thermodynamics of the aerosol system, the unification of the two particles lowers the energy of the system by reducing the surface area. For sufficiently small aerosol particles where other influences are not significant, experimental evidence[10] confirms the theoretical indications that the binary reaction constant analogous to k_{mn} is a coagulation rate and must be greater than the value given by the particles' geometrical cross sections alone, contrary to the case for colliding molecules.

Since clusters span the microscopic-macroscopic scale, their collisions are expected to show a corresponding range of characteristics. In the most general case, and particularly for very small clusters, questions of the disposal of collisional energy, rearrangement following collision, evaporation, and other questions are present which require treatment by simulation methods and are currently under investigation.[11] However, there are some important limiting cases for which these questions are secondary. One example is postcritical clusters in critical nucleation[12] where only clusters larger than a critical size are thermodynamically stable. The second case is where no barrier to nucleation exists such as for low-vapor-pressure monomers (i.e., where a molecular monomer can be thought of as the critical nucleus). In both cases, the interacting species resemble an aerosol in the sense that their coagulation rates k_{mn} are essentially the same as their collision rates. Thus, determination of the collision frequency alone is useful for a significant range of gas-phase clustering phenomena.

In collisions of thermalized, spherical aerosol particles, calculations show[9] that the total collision rates[13] are determined by the interaction potential energies of the particles at surface-to-surface separations greater than the 4-Å range where orbital overlap effects do not arise. Consequently, only the long-range components of the interaction energy need be considered for collisions. For molecules[14] these energies arise from van der Waals interactions and the interaction of the permanent moments of the molecules; for ultrafine particles, the permanent moments are assumed unimportant, leaving only the van der Waals–type interactions, whether they be the simple pairwise sum over intermolecular interactions or the collective interactions first discussed by Lifshitz,[15] to contribute to the long-range interaction potential energy.

The subject of this paper is the long-range potential between clusters. We will use a formulation of this energy that interpolates between the van der Waals energy for a pair of molecules and the collective energy that is appropriate for condensed-matter interactions. Calculations for a model case, identical pairs of $(CCl_4)_n$ clusters, will be performed and results compared with computationally simpler bulk-matter calculations. The domains of usefulness of the cluster and bulk computations will be discussed and practical computational approaches will be pointed out. While the immediate objective of these cal-

culations is the determination of the energies required for calculating gas-phase collision rates k_{mn}, the results are general in nature and should prove useful not only for describing the dynamics of gas-phase clusters but also in other cluster interaction questions and in more general questions where matter appears in quantities too small to be treated as "condensed" or "bulk" and too great to be adequately described as discrete atoms or molecules.

II. A CONSISTENT THEORY OF THE LONG-RANGE POTENTIAL BETWEEN CLUSTERS

While, in general, permanent moments are characteristics of most molecules, in this treatment we will not take their effects into consideration. This simplification is predicated upon the assumption that these moments, as well as characteristics of geometry, manifest themselves primarily in the particular structures of the cluster, a matter which is not the focus of these papers. Externally to the cluster, the aggregate effect of the permanent moments is largely cancelled due to the internal arrangement of the monomers. Thus, the fluctuating dipole–induced-dipole or London–van der Waals interaction is the lowest-order interaction energy that remains. For this reason, a description of this interaction, which applies with equal validity across all levels of atomic and molecular aggregation, is required and is the subject of this section, which in turn is the basis for the results of this paper.

A. Pair interactions

If perturbation theory is applied to solve a Schrödinger equation whose Hamiltonian is the lowest-order term in the expansion of the electrostatic interaction energy of two neutral atomic or molecular charge distributions[16] separated by a distance R, then the resulting "dispersion" energy is

$$\Delta E(R) = \frac{3e^4 h}{4\pi m^2 R^6} \sum_{m,n} \frac{f_{0m}^{(1)} f_{0n}^{(2)}}{\omega_{0m}^{(1)} \omega_{0n}^{(2)} (\omega_{0m}^{(1)} + \omega_{0n}^{(2)})} , \quad (1)$$

where e and m are the charge and mass of the electron, h is Planck's constant, and R is the separation of the centers of the two charge distributions. $f_{0n}^{(i)}$ is the oscillator strength of the ith molecule for the dipole transition between its ground state $|0\rangle$ and excited state $|n\rangle$ and $\omega_{0n}^{(i)}$ is the characteristic frequency of that transition.

Expressing the (isotropic) polarizability by

$$\alpha_i(\omega) = \frac{e^2}{m} \sum_n \frac{f_{0n}^{(i)}}{\omega_{0n}^{(i)2} - \omega^2} , \quad (2)$$

the resultant intermolecular energy is given as

$$\Delta E(R) = -\frac{3h}{(2\pi)^2 R^6} \int_{-\infty}^{\infty} \alpha_1(i\xi) \alpha_2(i\xi) d\xi \quad (3)$$

$$= -\frac{C_6}{R^6} , \quad (4)$$

where C_6 is defined by this expression and is the charac-

teristic parameter for the intermolecular van der Waals interaction.

If the assumption is made that the attractive interaction energy of aggregates of atoms or molecules can be computed as the pairwise a summation over the interaction energies of their constituents,[17] then the attractive energy of two bodies A and B can be expressed as

$$\Delta E_{AB} = -\int_{V_B} d\tau_B \int_{V_A} d\tau_A \frac{C_6 n_A n_B}{R^6} ,$$ (5)

where R is the separation distance between the volume elements $d\tau_A$ of A and $d\tau_B$ of B, C_6 is the van der Waals constant from Eq. (6) and n_A, n_B are the molecular number densities of volumes V_A and V_B. For the case of two spheres of radii a and b whose center-of-mass separation is R, the result of the integration is

$$\Delta E_{\text{sph}}^{AB} = -\frac{A_{AB}^{\text{H}}}{6} \left[\frac{2ab}{R^2-(a+b)^2} + \frac{2ab}{R^2-(a-b)^2} \right. \left. + \ln \left[\frac{R^2-(a+b)^2}{R^2-(a-b)^2} \right] \right] ,$$ (6)

where the constant A_{AB}^{H} is called the Hamaker constant and is defined as

$$A_{AB}^{\text{H}} = \pi^2 n_A n_B C_6 .$$ (7)

If the molecular species in A and B differ, C_6 is modified accordingly.

While Eq. (6) is mathematically simple, it suffers from two general defects: (1) As $R \to (a+b)$, $\Delta E_{\text{sph}}^{AB} \to -\infty$ rather than converging to a typical adhesion energy and (2) the integration in Eq. (5) does not take into account the collective effects that are operative in condensed matter (as discussed, for example, in Refs. 7 and 17). Thus, this treatment is inherently inconsistent and, as written, inappropriate for utilization in describing the interactions of clusters, even if rendered as a discrete summation.

B. Collective interactions

The long-range interaction energy of condensed bodies is computed analogously to that of the intermolecular energy discussed above. For condensed matter, the perturbations of the electrostatic interaction of the two bodies are their zero-point and thermal fluctuations.[15,18] The interaction energy arises from the dissipation[19] of these fluctuations and is dependent upon the frequency-dependent dielectric constants $\epsilon(\omega)$ of the bodies without direct reference to atomic or molecular structure. Unlike the pair-summation method, this approach intrinsically accounts for the collective effects that are present in condensed matter while not resolving the problem of divergence of the potential at particle contact.

The incorporation of the collective effects into the long-range force can be utilized to arrive at an alternative form for the Hamaker constant which is based strictly upon the properties of the interacting media. For interacting half-spaces A and B separated by a vacuum, the Lifshitz-Hamaker constant A_{AB}^{LH} can be expressed as[20]

$$A_{AB}^{\text{LH}} \approx \tfrac{3}{4} kT \left[\frac{\epsilon_A(0)-1}{\epsilon_A(0)+1} \right] \left[\frac{\epsilon_B(0)-1}{\epsilon_B(0)+1} \right]$$
$$+ \frac{3h}{8\pi^2} \int_{[(2\pi)^2 kT]/h}^{\infty} \left[\frac{\epsilon_A(i\xi)-1}{\epsilon_A(i\xi)+1} \right]$$
$$\times \left[\frac{\epsilon_B(i\xi)-1}{\epsilon_B(i\xi)+1} \right] d\xi .$$ (8)

Here, T is temperature, $\epsilon_A(i\xi)$ and $\epsilon_B(i\xi)$ are the dielectric constants on the imaginary frequency axis, and k is Boltzmann's constant. While this replacement is generally valid for half-spaces, for spheres it provides a lower bound on the magnitude of the Lifshitz–van der Waals energy[21] when used in Eq. (6).

Though the replacement of Eq. (7) by Eq. (8) is helpful in accounting for the collective intermolecular interactions characterizing condensed matter in the continuum limit, it does not indicate the manner in which the summed discrete interactions approach the condensed-matter interaction energy with increasing numbers of molecules, the question which is of interest for treating cluster interactions. This issue has been addressed directly by Langbein,[22] originally using a Drude oscillator model for the atoms. In this computation, the oscillators are coupled via the dipole coupling tensor

$$\mathsf{T}_{ij} = -\nabla_i \nabla_j \frac{1}{|\mathbf{r}_i - \mathbf{r}_j|} ,$$ (9)

where $\mathbf{r}_i$ is the location of oscillator i and the Hamiltonian for the coupled system is

$$H = \frac{m}{2} \sum_i (\dot{\mathbf{u}}_i^2 + \omega_i \mathbf{u}_i^2) = \frac{e^2}{2} \sum_{i \neq j} \mathbf{u}_i \mathsf{T}_{ij} \mathbf{u}_j .$$ (10)

Here, $\mathbf{u}_i$ and ω_i are, respectively, the oscillation amplitude vector and unperturbed frequency of oscillator i. The dispersion energy of this system is the difference between the zero-point energies of the coupled and uncoupled system of oscillators:

$$\Delta E = \frac{h}{4\pi} \sum_i (\Omega_i - \omega_i) ,$$ (11)

where, here, Ω_i are the coupled eigenfrequencies. Again, using perturbation methods, Langbein gave a series solution to this problem and showed that by assuming the standard Clausius-Mossotti relation between the dielectric constant and the molecular polarizability, he could derive the Lifshitz energy.[15]

This formulation of the coupled interaction energy, which reduces to the pair-interaction energy in the limit of two oscillators (or molecules) and to the condensed-matter form in the limit of a highly coupled system, suggests that it is the proper framework for calculating cluster interaction energies where a limited number of oscillators interact. For the coupling of discrete oscillator units, the total energy may be shown[23,24] to be expressed as

$$(\Delta E_{AB})_{\text{tot}} = \frac{h}{8\pi^2} \int_{-\infty}^{\infty} d\xi \ln\{\det[\underline{I} - \alpha(i\xi)\mathsf{T}]\} ,$$ (12)

where

$$\alpha(i\xi) = \begin{bmatrix} \alpha^{(A)} & 0 \\ 0 & \alpha^{(B)} \end{bmatrix} \tag{13}$$

is the polarizability matrix for the system and $\underline{I}$ is the $3N_A \times 3N_B$ identity matrix, with N_x the number of molecules in cluster x. Each major submatrix $\alpha^{(x)}$ is diagonal in the 3×3 polarizability tensors, each of which corresponds to a distinct molecule in cluster X. The dipolar coupling tensor

$$\mathsf{T} = \begin{bmatrix} \mathsf{T}^{(A)} & \mathsf{T}^{(C)} \\ \mathsf{T}^{(C)} & \mathsf{T}^{(B)} \end{bmatrix} \tag{14}$$

consists of the submatrices given by Eq. (9) where the indices are such that $\mathsf{T}^{(A)}$ couples only molecules in A, $\mathsf{T}^{(B)}$ couples only molecules in B, and $\mathsf{T}^{(C)}$ couples the molecules in the separate clusters. The cluster interaction energy ΔE_{AB} is given as the difference between the energy of the fully coupled clusters and the sum of the individual cluster self-energies in isolation of each other [i.e., Eq. (12) with $\mathsf{T}^{(C)}$ set to 0],

$$\Delta E_{AB} = (\Delta E_{AB})_{\text{tot}} - (\Delta E_A + \Delta E_B) \ . \tag{15}$$

The energy as represented by Eq. (15) is the basis for computing the long-range cluster interaction energies in this paper. While it is a relatively crude representation for general intracluster properties, for intercluster attraction, it should be realistic provided no collective states, such as conduction bands, form within the clusters.

III. LONG-RANGE INTERACTION ENERGY CALCULATIONS: CCl₄ CLUSTERS AS PROTOTYPE

A. Molecular parameters

Carbon tetrachloride was chosen for the calculations of this and the subsequent paper on the collision frequency for several reasons: (1) The approximately spherical symmetry of the individual molecules reduces the need for including permanent moments and molecular structural features in energy calculations and structures of the clusters. (2) An extensive literature on the substance facilitates accurate polarizability[25] and dielectric-constant determinations from spectroscopic data. (3) Unlike the rare-gas atoms for which calculations of idealized cluster systems are often performed, a molecular species possesses infrared and longer-wavelength polarizability which can materially affect collisions,[9] the immediate application for these studies.

Quasispherical clusters are used as the subject of this study to facilitate comparison between microscopic and macroscopic calculations of energy and collisions. Since we want to compare cluster energy calculations with the results from Lifshitz theory, results must be available from that continuum theory in a geometry that corresponds to the geometrical arrangement utilized for the clusters. For the collisions, exact transport formulas that can be used as the basis for approximate treatment of cluster collisions are available only for spheres.

The programs for computing Eqs. (12) and (15) were written in FORTRAN for an IBM-3090 computer located at Texas A & M University. It is adapted for IBM main frames because it uses IBM-SL mathematical subroutines.[26] These subroutines, along with IMSL subroutines[27] also utilized, are vectorized along with the rest of the code during compilation of the FORTRAN source file. Throughout, double precision is employed for all real variables.

For both the purposes of deriving interaction energies for clusters that assume physically realistic forms and for determining the minimal energy configurations of the clusters (assuming no internal degrees of freedom for the purposes of this calculation), a short-range repulsive intermolecular potential has been used. A Lennard-Jones (n-6) type potential has been taken with the following form (Ref. 16, pp. 28 and 29):

$$\begin{aligned} V(r) &= -\frac{C_6}{r^6} + \frac{C_n}{r^n} \\ &= -V_0 \left[\frac{n}{n-6} \left(\frac{\sigma}{r} \right)^6 - \frac{6}{n-6} \left(\frac{\sigma}{r} \right)^n \right] , \end{aligned} \tag{16}$$

where r is the separation distance between the centers of mass of the two molecules, n is a variable integer, V_0 is the extremum of the potential, and C_6 and C_n are the corresponding potential constants, with C_6 given by Eq. (3). Most recently, CCl₄ has been referred to as having a (24-6) potential[28,29] so that

$$\begin{aligned} V(r) &= -\frac{C_6}{r^6} + \frac{C_{24}}{r^{24}} \\ &= -\frac{V_0}{3} \left[4 \left(\frac{\sigma}{r} \right)^6 - \left(\frac{\sigma}{r} \right)^{24} \right] . \end{aligned} \tag{17}$$

The unknown quantity C_{24} can be found from the knowledge of C_6 and σ, which are empirical quantities. Using the dynamic polarizability[25] in Eq. (3) gives the value $C_6 = 3.110 \times 10^{-57}$ erg cm⁶. The value of σ, which can also be considered as the spherical molecule diameter, is obtained from the literature[30] as 5.77 Å. At contact the relation $C_{24} = (C_6\sigma^{18})/4$ holds, which yields

$$(C_{24})^{1/24} = 1.554 \times 10^{-8} (\text{erg cm}^{24})^{1/24} .$$

From this value and C_6, the value of $|V_0|$ is found to be 6.321×10^{-14} erg, which is comparable to well depths found in the literature. In one case,[31]

$$|V_0| = 4.418 \times 10^{-14} \text{ erg}$$

for $\sigma = 5.753$ Å and in another,[29]

$$|V_0| = 8.384 \times 10^{-14} \text{ erg}$$

for $\sigma = 5.806$ Å. Thus, the computation of C_6 from the dynamic polarizability is entirely consistent with data from other sources.

In a direct check on the computational procedure employed here, Eq. (12) as formulated in the general case for utilization in cluster coupling was computed for the case of a pair of interacting molecules. A deviation in C_6 of

less than 0.25% from the value given by computing Eq. (3) was found implying only a 0.01% difference between the resultant recomputed C_{24} and the value computed above.

In the following calculations, the r^{-24} repulsive intermolecular potential is assumed to be pairwise additive for an assembly of N molecules, unlike the coupling for the van der Waals attraction. Therefore, the repulsive part of the total interaction of such a system is given by

$$\Delta E_{\text{rep}} = \sum_{i>j}^{N} \sum_{i,j=i}^{N} \frac{C_{24}}{r_{ij}^{24}} , \qquad (18)$$

where r_{ij} is the separation between the centers of molecules i and j. In the case of an interaction-energy computation between two molecular clusters A and B, only the terms coupling pairs, with one molecule located in A and the other one in B, need to be summed.

B. Structure of the clusters

In order to assemble the most compact clusters feasible for comparison with spheres described via a continuum picture of matter, we selected the 13-molecule icosahedron as the starting point. It consists of a central molecule with 12 first-layer molecules arranged about it at equal distances from each other. Around this first layer, a second layer of molecules was assembled in two ways. In the first arrangement, a 33-molecule, dodecahedral cluster was constructed by placing a molecule in contact with each of the 20 triplets of first-layer neighbors. In the second arrangement, the second layer was assembled around the icosahedral core by adding one molecule at the top of each of the 12 first-layer elements (i.e., on the straight line passing through the centers of the core and first-layer molecules) and one in contact with each of the 20 pairs of first-layer neighbors to give a 55-molecule isosahedron. Experimental measurements of the size distributions of clusters have pointed to the existence of "magic" numbers corresponding to the numbers of molecules in particularly stable clusters. The numbers of elements required to build icosahedrons (13,55,147,309,...) were found to be magic, confirming the strong stability of icosahedral structures. The 33-molecule dodecahedron is used because it provides a high-symmetry cluster intermediate between the two lowest icosahedrons for comparison with continuum calculations.

The configuration of greatest stability, or lowest interaction potential energy (not free energy), is obtained by taking account of the many-body induced polarization, Eq. (12), which lowers the potential along with the positive, repulsive potential of Eq. (18). In the three cases, the outer cluster molecules are assumed to have the same size as if they were isolated because they are the ones that are the least affected by van der Waals force compression. Thus, for carbon tetrachloride, the outer hard sphere elements will be assumed to measure $2R = 5.77$ Å in diameter. Then half the distance between first-layer neighbor molecules is chosen as the packing variable. It is noted r and represents the unit distance factor which the normalized coordinates of the 13-molecule icosahedron vertices have to be multiplied to be
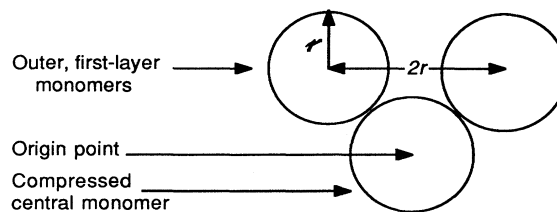

FIG. 1. Segment from 13-molecule icosahedron illustrating notation. Distance between first-layer neighbors, $2r$, is variable used in search for minimum-energy configuration of cluster and r' is radius of first-layer molecules for the resulting structure. For 13-molecule icosahedron, first-layer molecules are also outer-layer molecules so that $r' = R = 2.885$ Å. R is half the center-of-mass separation between molecules in an isolated pair.

expressed in real scale. For every packing variable step, the locations of the molecules within the cluster are determined from the geometrical constraints defining the clusters. Once the spatial coordinates of a cluster's molecules are given, the self-energy is then calculated on the basis of Eq. (12) to which the repulsive potential given by Eq. (18) is added and for 55-molecule cluster results in a modified radius r' for the first-layer molecules. See Fig. 1.

1. The 13-molecule icosahedron

A molecule is first located at the origin point while the twelve others are distributed at the vertex sites of the icosahedron, with the real scale factor r varying by incrementation: The packing variable r is initialized to the value R, that is to say, half the distance at contact between outer layer molecules, and then incremented before
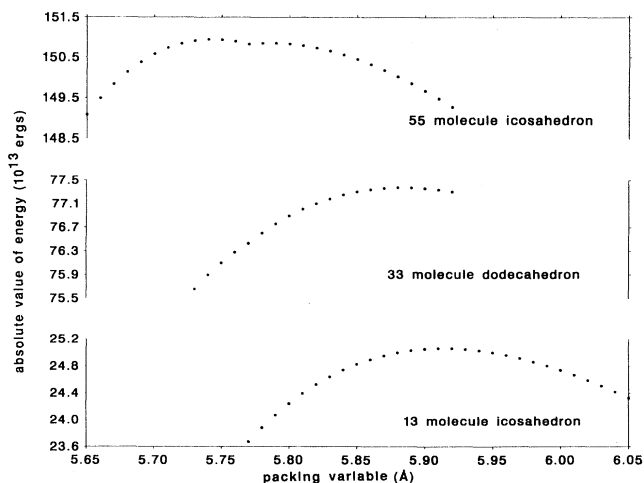

FIG. 2. Absolute value of cluster self-energy from Eq. (12) as a function of packing variable r for 13-, 33-, and 55-molecule carbon tetrachloride icosahedral and dodecahedral clusters.

each potential-energy computation until the minimum has clearly been reached indicating the most stable packing. Due to the geometry defining the cluster, the central sphere undergoes compression even though the outer molecules are not in contact with one another. Figure 2 shows the absolute value of the cluster energy versus the distance between vertex-center neighbors for the 13 carbon tetrachloride element icosahedron. It exhibits the energy extremum at

$$E_{min} = -25.06 \times 10^{-13} \text{ erg}$$

for a separation distance between two close vertex molecules of $2r = 5.91$ Å. With the assumption above concerning the size of the outer surface molecules, the radius r' of the molecules in the first layer has the value $R = 2.885$ Å giving a diameter of 5.47 Å for the central sphere molecule, representing a 5.17% compression in radius.

2. The 33-molecule dodecahedron

The same process is used, but the way the packing variable is incremented requires modification. Because of the addition of a second layer of molecules upon the 13-molecule icosahedron, the 33-molecule dodecahedron should increase the van der Waals forces packing around the central sphere molecule, therefore decreasing the distance between first-layer neighbors when reaching minimum energy. So this time, for each energy computation step, the packing variable r must be decremented from a value only slightly greater than the one corresponding to the most stable packing in the 13-molecule configuration. While the locations of the 12 first-layer molecules are still determined by the simple prescription for the icosahedron vertex coordinates, the coordinates of the 20 second-layer molecules are somewhat more complex because they are derived from the locations of three molecules in the first layer. Figure 2 displays the self-energy of the 33-molecule dodecahedron. It reveals the energy extremum at

$$E_{min} = -77.38 \times 10^{-13} \text{ erg}$$

for an inner-layer neighbor separation distance of $2r = 5.88$ Å. Since this distance is greater than $2R$, for a stable packing, the inner-layer neighbor elements are not in contact with one another, so they undergo no compression according to the above assumption. Because of the assumption, too, the graph shows a slight curve discontinuity at $2r = 5.77$ Å. With $r = 2.94$ Å and $r' = 2.885$ Å, the diameter of the central sphere is 5.415 Å, which represents a reduction in radius of 6.16%.

3. The 55-molecule icosahedron

As in the preceding case, to identify the minimal-energy structure of the 55-molecule icosahedron, the packing variable r was decremented for each stage of computation. In this case, the final configuration was not a true icosahedron due to a misalignment of the three outer-layer elements with the 13-element icosahedron below. The results for this calculation are displayed in

Fig. 2. As for the dodecahedron, the discontinuity at $2r = 5.77$ Å is due to the assumption of no modification of molecular radius for the outer-layer molecules. The minimum cluster self-energy is found at

$$E_{min} = -150.95 \times 10^{-13} \text{ erg}$$

for an inner-layer neighbor separation distance of $2r = 5.74$ Å. Since this $2r$ value is smaller than $2R$, r' here equals r, and the first-layer molecules undergo a slight reduction due to compression. Their diameter is decreased by 0.52%, whereas that of the central sphere is found to be 5.18 Å, a reduction of 10.26%.

C. Interaction energies for pairs of clusters

1. Choice of orientations and averaging

The absence of spherical symmetry for real clusters necessitates the selection of specific relative orientations for which interaction energies are to be calculated. Since a primary objective of this study is the determination of the approach of the long-range interaction energy of clusters to that of spheres treated as bulk matter, cluster relative orientations are used which bracket the possible range of interaction energies. Thus for each type of cluster, the only cases of interaction orientation that are studied are the "extreme" mutual configurations which in terms of center-of-mass separation distance at contact are those orientations at which the separations are greatest and least. However, any mutual configuration for which the clusters' outer molecules would fit into one another at contact is ignored because such a case corresponds neither to any possible interaction of distinct, macroscopic spheres nor to a configuration relevant to computations of total collision frequency.

For the icosahedrons, energies are computed for two relative orientations that can be described as mirror symmetric. The first orientation brings the clusters together along their threefold axes of symmetry to provide the orientation giving the distance of closest approach of the centers of mass. In the second case, the clusters approach along their fivefold axes giving the greatest center-of-mass separation distances with only one molecule from each cluster coming in contact. For the first case, two triangles of molecules face each other directly in the 13-molecule example and six elements face each other in the 55-molecule example.

In the same way for the 33-molecule dodecahedron, the threefold and fivefold axes in mirror symmetry are utilized. This time, the clusters' centers of mass are closer at contact when interacting along their fivefold axis, where pentagons of molecules face each other; in contrast, the dodecahedrons are more distant when facing each other along their threefold axis where single molecules only approach each other.

Due to the dependences of the interaction energies on the relative orientations of the discrete clusters, comparison with the Lifshitz-Hamaker result for spheres requires an averaging of the cluster energies. The objective of the following approach to averaging is intended to pro-

TABLE I. Cluster diameters.

n	13		33		55	
r (Å)	2.957		2.942		2.872	
Type	13S3	13S5	33S3	33S5	55S3	55S5
d_{clust} (Å)	14.71	17.02	23.99	20.25	23.77	28.21

vide a rough approximation for the sake of comparison and not necessarily as the basis for a general approximation for the effects of orientationally dependent long-range interactions on collision dynamics. For each of the three cluster interactions, a rotationally averaged potential is computed from the limit-case potentials computed for the clusters. This averaging was accomplished by taking the degrees of degeneracy of the chosen mutual orientations as weighting factors for averaging. The three clusters under study have 12 fivefold axes and 20 threefold axes so the mean potential is computed for values of the intercluster distances greater than the largest contact separations as the weighted average

$$\Delta E_{\text{av}} = (20 \Delta E_{\text{threefold}} + 12 \Delta E_{\text{fivefold}}) / 32 \ . \tag{19}$$

The "diameter" of a cluster, used to define the center-of-mass separation at closest approach of the clusters, is given by a surface-molecule radius, plus the projection onto the line between the centers of the two clusters of the position vector of one of the surface molecules that is nearest a surface molecule in the opposing cluster. Symbolically, the diameter is given by

$$d_{\text{clust}} = 2(\mathbf{u} \cdot \mathbf{x}_{\text{out}} + R) \ , \tag{20}$$

where $\mathbf{u}$ is the unit vector orienting the direction of the interaction, $\mathbf{x}_{\text{out}}$ is the location vector of one of the outer-layer molecules sitting on or next to the axis oriented by $\mathbf{u}$, and $R = 2.885$ Å. Table I gives the values defining the clusters and their diameters where r is the packing variable, nSm represents the cluster pair with n molecules in each cluster aligned such that the m-fold axes of symmetry for the two clusters coincide and provide the axis of symmetry for the pair of clusters (i.e., the clusters are in mirror symmetry).
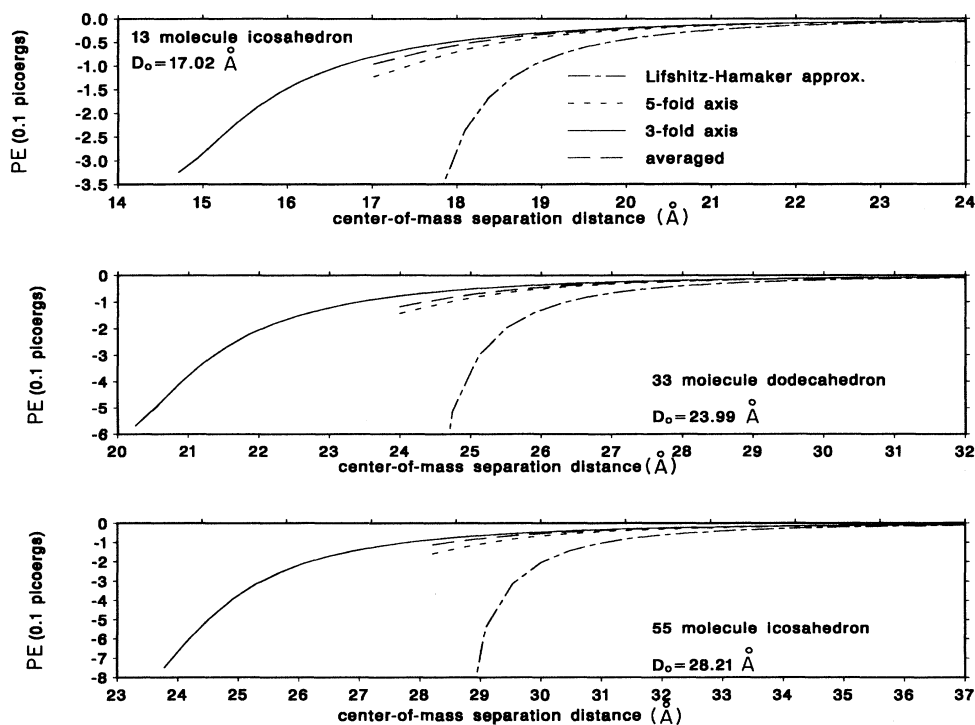

FIG. 3. Interaction potential energies (PE) plotted as functions of center-of-mass separation for three identical pairs of carbon tetrachloride clusters where D_0 is the diameter of sphere circumscribed about single cluster: Lifshitz-Hamaker approximation from Eq. (6); fivefold axis and threefold axis from Eq. (15) with clusters in mirror-symmetric orientation along respective axes, averaged from Eq. (19).

2. Discrete-cluster interaction-energy results

Cluster interaction energies were calculated for the six orientations discussed above at a sequence of separations adequate to determine a spline fit of order 7 to the energies.[32] Figures 3(a)–3(c) display the values that were determined with the relative orientations as discussed above indicated on the graphs. On each of these graphs the dotted lines that start at the center-of-mass separations d_{clust}, as given in Table I, represent the two limiting-case energies computed from eqs. (12)–(15) with the rotationally averaged potential generated from them; the solid lines correspond to the potentials obtained from Lifshitz theory via Eqs. (6) and (8).

Several observations can be made on the energies graphed Figs. 3(a)–3(c). At contact, the interactions along the threefold axes for the iosahedrons and fivefold axis for the dodecahedron are much stronger than the energies at contact along the other axes where only single molecules face each other. The contact-energy difference between the two types of orientations increases with the number of molecules facing one another, which is to be expected. Next, consider cluster interaction energy for center-of-mass separations greater than the smaller of the two values of d_{clust} given in Table I for each pair of clusters. The interaction energy for the clusters in the orientation with the smaller d_{clust} value decreases sufficiently rapidly with increasing separation that when it is equal to the larger of the d_{clust} values, the energy is smaller than the contact energy for the orientation with only single molecules facing each other. This is due to the rapid decrease in energy with distance of separation that leaves the nearest molecules as dominating the interaction for a given center-of-mass separation. Finally, at relatively long range, the two interaction potential types converge on each of the three graphs: If we take r^* as the center-of-mass separation distance in units of the diameter of either cluster in each pair, then the two energy values differ by less than 15% for $r^* = 1.2$ and less than 9% for $r^* = 1.3$. This observation is in agreement with the picture that clusters lose their discrete-molecule interaction aspect as they become sufficiently removed from each other.

3. Macroscopic-sphere interaction

For the purpose of comparing the interaction energies of the clusters of discrete molecules with energies based upon a continuum model of the clusters, a macroscopic sphere of radius D_0 which approximates a cluster is defined as that sphere which circumscribes the cluster; D_0 is equal to the larger of the two values of d_{clust} for each set of clusters in Table I.

While a temperature-dependent form of the Lifshitz-Hamaker constant, Eq. (8), is expressed here for correctness, its value for carbon tetrachloride is essentially the same as for the zero-temperature limit. For cases in which $\epsilon(i0) \neq \epsilon(i2\pi kT/\hbar)$, the finite-temperature form of Eq. (12) (see Ref. 24, p. 37) must be employed.

The number densities used to compute the dielectric susceptibilities from the dynamic polarizability[25] were consistent with the packing of the clusters considered here. For each of the three cluster structures studied, the number density was found by dividing the number N_1 of molecules within the cluster by the volume $V = (4\pi/3)(D_0/2)^3$ of the corresponding circumscribed sphere. Thus, because of the variations of such ratios, the dielectric and Lifshitz-Hamaker constants were found to have values somewhat different from the one found for the liquid phase at normal temperature and pressure. Table II presents these data.

For the purpose of comparing the Lifshitz-Hamaker potential with the microscopic potential, the rotationally averaged potential based upon discrete interactions is assumed to approach most closely to the macroscopic case while best reflecting the exact energy. Therefore, for brevity, it will be referred to as the discrete potential. Referring again to Figs. 3(a)–3(c), at very short range, the Lifshitz-Hamaker energy is far from the discrete potential and is a manifestation of the divergence at contact implicit in Eq. (6). At longer range $(1.5 < r^* < 2)$, the continuum approximation leads to energies close to the discrete ones, and then matches them around $r^* = 2$, and subsequently slightly underestimates them, as is anticipated by the fact that it is lower bound, as mentioned above. Quantitatively, the underestimate for $r^* > 2$ is by less than 15% for r^* going to infinity. This is shown in Fig. 4, which represents the relative difference between the Lifshitz-Hamaker and discrete potentials $[\Delta = (E_{\text{LH}} - E_{\text{av}})E_{\text{av}}]$ versus the ratio $r^* = D/D_0$, where D is center-of-mass separation and D_0 varies according to the individual case as given in Table II. The relative match of the two potentials at long range comes into agreement again with the fact that clusters, by losing their discrete aspect when remote enough from each oth-

TABLE II. Parameters used for the computation of the Lifshitz-Hamaker potential.

	Liquid at 20 °C[a]	13-molecule cluster	33-molecule cluster	55-molecule cluster
Circumscribed sphere diameter D_0 (Å)		17.02	23.99	28.21
Number density (nm^{-3})	6.23	5.037	4.564	4.679
Dielectric constant ϵ	2.238	1.928	1.817	1.843
A_{AB}^{LH} (10^{13} erg)	9.919	6.698	5.572	5.838

[a]Bulk properties are given for comparison; cluster structures were chosen soley to facilate studies of current and following papers so there is no reason to expect cluster physical properties given in this table to converge to the properties of the bulk substance.
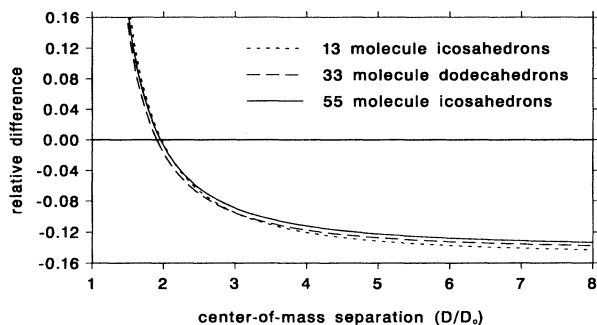
FIG. 4. Relative difference $\Delta = (E_{LH} - E_{av}/E_{av}$, between continuum-model attractive energy E_{LH} according to Eq. (6) and rotationally averaged energy E_{av} from Eq. (19) for discrete clusters plotted as a function of nondimensionalized center-of-mass separations D/D_0.

er, can be treated as bulk-matter spheres. This macroscopic view is confirmed by the observation that at quite long range $(r^* > 4)$, the larger the interacting clusters are, the closer their Lifshitz-Hamaker potential matches the exact potential.

IV. CONCLUSIONS AND IMPLICATIONS

The fact that the energy following from the use of the Lifshitz-Hamaker constant in Eq. (6) exceeds the iterated induced-dipole energy for $r^* < 2$ indicates that at close range the approximation implicit in the macroscopic, or continuum picture, fails for small clusters. At very close range where orbital overlap enters, the omission of the repulsive interaction should play a role. However, the

fact that discrete and continuum potentials become comparable at the same *scaled* separation, as opposed to the same actual distance, indicates the deficiency in the continuum picture for separations $(D_0 + 1 \text{ Å})/D_0 < r^* < 2$ lies less in the absence of the repulsive term than in the substitution of an averaged picture of the interaction for what is intrinsically the cumulative energy of discrete interactants. Another way of viewing this energy is to consider the relative difference curves of Fig. 4 as functions of actual, not scaled, separation. In that case, the convergence of the discrete to the continuum energies occurs at distances that increase with the size of the cluster, thereby indicating that, prior to the apparently asymptotic convergence of discrete to continuum for $r^* > 4$, the relation of separation to particle dimension is important.

The meaning of these energy calculations for describing physical results is dependent upon application. Implicit to what is calculated here is the interaction of geometrically delimited media. Thus, no conclusions for interacting half-spaces and adhesion energies for thick films according to Lifshitz theory are clear from these calculations. In contrast, for spreading films, there may be a benefit from describing the leading edge of the film in terms of discrete interactions, as is done here. Similarly, in colloidal considerations, calculation of micellar long-range interactions are very much subject to the questions treated here. Applications of these results to collisions of gas-phase clusters are treated in the following paper.[1]

*Author to whom correspondence should be addressed.

[1]A. S. Amadon and W. H. Marlow, following paper, Phys. Rev. A **43**, 5493 (1991).

[2]R. D. Levine and R. B. Bernstein, *Molecular Reaction Dynamics and Chemical Reactivity* (Oxford University Press, New York, 1987).

[3]G. M. Hidy and J. R. Brock, *The Dynamics of Aerocolloidal Systems* (Pergamon, New York, 1970), p. 119.

[4]J. G. Gay and B. Berne, J. Colloid Interface Sci. **109**, 90 (1986).

[5]W. H. Marlow, in *Proceedings of the Coagulation Workshop, Karlsruhe, 1988*, edited by: G. Metzig and W. O. Schikarski (Kernsforschungzentrum Karlsruhe GmbH, Karlsruhe, 1989).

[6]W. H. Marlow, in *Aerosol Microphysics I: Particle Interaction*, edited by W. H. Marlow (Springer-Verlag, Berlin, 1980), Chap. 1.

[7]W. H. Marlow, in *Aerosol Microphysics I: Particle Interaction* (Ref. 6), Chap. 5.

[8]N. A. Fuchs and A. G. Sutugin, J. Colloid Interface Sci. **20**, 492 (1965).

[9]W. H. Marlow, J. Chem. Phys. **73**, 6288 (1980).

[10]K. Okuyama, Y. Kousaka, and K. Hayashi, J. Colloid Interface Sci. **101**, 98 (1984).

[11]R. R. Lucchese and W. H. Marlow, in *On Clusters and Clus-*

tering: From Atoms to Fractals, edited by D. Nelson and P. Reynolds (North-Holland, Amsterdam, in press).

[12]F. F. Abraham, *Homogeneous Nucleation Theory* (Academic, New York, 1974).

[13]W. H. Marlow, J. Chem. Phys. **73**, 6284 (1980).

[14]H. Margenau and N. R. Kestner, *Theory of Intermolecular Forces*, 2nd ed. (Pergamon, New York, 1970).

[15]E. M. Lifshitz, Zh. Eksp. Teor. Fiz. **29**, 94 (1955) [Sov. Phys.–JETP **2**, 73 (1956)].

[16]C. Maitland, M. Rigby, E. B. Smith, and W. A. Wakeham, *Intermolecular Forces: Their Origin and Determination* (Clarendon, Oxford, 1987), pp. 57–71.

[17]J. Mahanty and B. W. Ninham, *Dispersion Forces* (Academic, New York, 1976), pp. 9–22.

[18]I. E. Dzyaloshinskii, E. M. Lifshitz, and L. P. Pitaevskii, Adv. Phys. **10**, 165 (1961).

[19]H. B. Callen and T. A. Welton, Phys. Rev. **83**, 34 (1951).

[20]J. N. Israelachvili, *Intermolecular and Surface Forces* (Academic, London, 1985), p. 142.

[21]D. Langbein, J. Phys. Chem. Solids **32**, 1657 (1971).

[22]D. Langbein, J. Phys. Chem. Solids **32**, 133 (1971).

[23]J. Mahanty and B. W. Ninham, *Dispersion Forces* (Academic, New York, 1976), p. 29.

[24]D. Langbein, *Van der Waals Attraction* (Springer-Verlag, Ber-

lin, 1974).

[25]A. S. Amadon and W. H. Marlow, J. Colloid Interface Sci. (to be published).

[26]*IBM Engineering and Scientific Subroutine Library Guide and Reference, Release 3,* 4th ed. (IBM, Armonk, NY, 1988), p. 381.

[27]*IMSL Math/Library: Fortran Subroutines for Mathematical Applications* (IMSL, Houston, 1987).

[28]J. Fisher, R. Lusting, H. Breitenfelder-Manske, and W. Lem-ming, Mol. Phys. **52**, 485 (1984).

[29]R. Lustig, Fluid Phase Equilibria **32**, 117 (1987).

[30]F. Serrano Adnan, A. Bañon, and J. Santamaria, Chem. Phys. Lett. **107**, 475 (1984).

[31]J. Samios and T. Dorfmuller, J. Chem. Phys. **76**, 5463 (1982).

[32]*User's Manual, IMSL Math/Library: Fortran Subroutines for Mathematical Applications* (IMSL, Houston, 1989). Spline interpolation algorithims DBSINT, DSNAK, pp. 436–442.